J. Biochem. 2009;145(5)685–691
doi:10.1093/jb/mvp026

Intramolecular Electron Transfer Processes in Cu_B-deficient Cytochrome *bo* Studied by Pulse Radiolysis

Kazuo Kobayashi[1], Seiichi Tagawa[1] and Tatsushi Mogi[2,3,*]

[1]Institute of Scientific and Industrial Research, Osaka University, Mihogaoka, Ibaraki, Osaka 567-0047; [2]ATP System Project, ERATO, JST, Nagatsuta 5800-2, Midori-ku, Yokohama 226-0026; and [3]Department of Biomedical Chemistry, Graduate School of Medicine, the University of Tokyo, Hongo, Bunkyo-ku, Tokyo 113-0033, Japan

Received December 25, 2008; accepted February 6, 2009; published online February 13, 2009

The *Escherichia coli* cytochrome *bo* is a heme-copper terminal ubiquinol oxidase, and functions as a redox-driven proton pump. We applied pulse radiolysis technique for studying the one-electron reduction processes in the Cu_B-deficient mutant, His333Ala. We found that the Cu_B deficiency suppressed the heme *b*-to-heme *o* electron transfer two order of the magnitude ($4.0\times10^2\ s^{-1}$), as found for the wild-type enzyme in the presence of 1 mM KCN ($3.0\times10^2\ s^{-1}$). Potentiometric analysis of the His333Ala mutant revealed the 40 mV decrease in the E_m value for low-spin heme *b* and the 160 mV increase in the E_m value of high-spin heme *o*. Our results indicate that Cu_B not only serves as one-electron donor to the bound dioxygen upon the O-O bond cleavage, but also facilitates dioxygen reduction at the heme-copper binuclear centre by modulating the E_m value of heme *o* through magnetic interactions. And the absence of a putative OH^- bound to Cu_B seems not to affect the uptake of the first chemical proton *via* K-channel in the His333Ala mutant.

Key words: copper B mutant, cytochrome *bo*, electron transfer, pulse radiolysis, quinol oxidase.

Abbreviations: NMA, *N*-methylnicotinamide; Q_H, the high-affinity quinone-binding site; Q_L, the low-affinity quinol-oxidation site; Q_n, ubiquinone-*n*; Q_nH_2, ubiquinol-*n*; SML, sucrose monolaurate.

Cytochrome *bo* (CyoABCD) is a heme-copper terminal ubiquinol oxidase in the aerobic respiratory chain of *Escherichia coli*, and predominantly expressed under highly aerated growth conditions (*1–3*). Subunit I (CyoB) binds all four bound redox centres, the high-affinity ubiquinone binding site (Q_H[1]), low-spin heme *b*, high-spin heme *o* and Cu_B and the latter two centres form the heme *o*-Cu_B binuclear metal center (*1–4*). Quinols are oxidized at the low-affinity quinol oxidation site (Q_L) in subunit II (*5–7*), and electrons are sequentially transferred through Q_H and heme *b* to the binuclear centre (*8–11*), where dioxygen reduction takes place. The two-electron oxidation of ubiquinol-8 (Q_8H_2) at the periplasmic side of the cytoplasmic membrane is coupled to the four-electron reduction of dioxygen to water at the cytoplasmic side. Accordingly, four chemical protons are apparently translocated from the cytoplasm to the periplasm, generating an electrochemical proton gradient across the membrane. In addition, by a pump mechanism, it can vectorially translocate four other protons per dioxygen reduction. Site-directed mutagenesis (*12–15*) and X-ray crystallographic (*4*, *16–18*) studies on bacterial heme-copper terminal oxidases suggest that D- and K-channels in subunit I are operative during redox-coupled proton pumping. Uptake and release of protons and intramolecular proton transfer in the oxidase appear to be coupled to electron transfer processes (*19*, *20*).

*To whom correspondence should be addressed. Tel: +81 3 5841 8202, Fax: +81 3 5841 3444, E-mail: tmogi@m.u-tokyo.ac.jp.

In the structure of cytochrome *bo*, the bound quinone, heme *b*, heme *o* and Cu_B are sequentially placed in subunit I (*4*). At the distal end of the electron transfer pathway, Cu_B serves as a transient ligand binding site during the delivery of exogenous ligands to the high-spin heme (*21–22*), and also as a one-electron donor to dioxygen bound to heme *o* (heme a_3 in cytochrome *c* oxidase) for the O-O bond cleavage. One of three Cu_B ligand histidines, His284, forms a N_ε-C_ε covalent bond with Tyr288 (*23*, *24*), and the cross-linked Tyr288 facilitates the O-O bond scission by hydrogen transfer to the bound dioxygen (*25–29*).

Pulse radiolysis is a powerful tool for investigating electron transfer process within proteins, often allowing an electron to be introduced rapidly and selectively into one redox center of enzymes (*11*, *30–35*). Here we applied pulse radiolysis to the Cu_B-deficient mutant His333Ala (*36*), in order to investigate the effects of the Cu_B deficiency on the one-electron reduction processes in the resting oxidized enzyme. We found that a lack of Cu_B altered the E_m values of both low-spin heme *b* and high-spin heme *o*, and reduced the heme *b*-to-heme *o* electron transfer two-order of magnitude.

MATERIALS AND METHODS

Enzyme Preparations—The wild-type enzyme and the Cu_B-deficient mutant His333Ala were isolated from the cytochrome *bo*-overproducing strains GO103/pHN3795-1 (*cyo*$^+$ Δ*cyd*/*cyo*$^+$) and ST4533/pHN3795-H333A (Δ*cyo cyd*$^+$/*cyo*), respectively, as described previously (*36*, *37*).

Pulse Radiolysis—Pulse radiolysis experiments were performed under anaerobic conditions with a linear accelerator at the Institute of Scientific and Industrial Research, Osaka University (*11*, *30–34*). The pulse width and energy were 8 ns and 27 MeV, respectively. The sample was placed in a quartz cell with an optical path length of 0.2 or 1 cm. The temperature of the sample was maintained at 25°C. The enzyme solution contains 10 mM sodium acetate buffer (pH 5 to 6), 10 mM potassium phosphate (pH 6 to 8) or 10 mM sodium borate buffer (pH 8 to 10) containing 0.1% sucrose monolaurate (SML; Mitsubishi-Kagaku Foods Co., Tokyo) and 2 mM NMA. The concentration of NMA radicals generated by pulse radiolysis was adjusted by varying the dose of the electron beam. The spectral data after the first or the second pulse were collected, since many pulses inflict damage on protein.

Potentiometric Titrations—Spectroscopic titrations were performed essentially as described by Dutton (*38*), using a Hitachi U-3000 spectrophtometer and a custom-made anaerobic cuvette. The oxidized enzyme in 20 mM potassium phosphate buffer (pH 7.4) containing 1.0% *n*-octyl-β-D-glucoside was mixed with redox mediators; potassium ferricyanide ($E_m = +430$ mV), quinhydrone ($E_m = +280$ mV), 1,2-naphthoquinone ($E_m = +143$ mV), phenazine methosulfate ($E_m = +80$ mV), duroquinone ($E_m = +10$ mV), 2-hydroxy-1,4-naphthoquinone ($E_m = -145$ mV), and riboflavin ($E_m = -390$ mV). Reductive titration was performed anaerobically at 20°C by addition of small aliquots of 5 mM sodium dithionite; for subsequent oxidative titration, 5 mM potassium ferricyanide was used as a titrant. Changes in absorbance at 428 nm were corrected with the dilution effect.

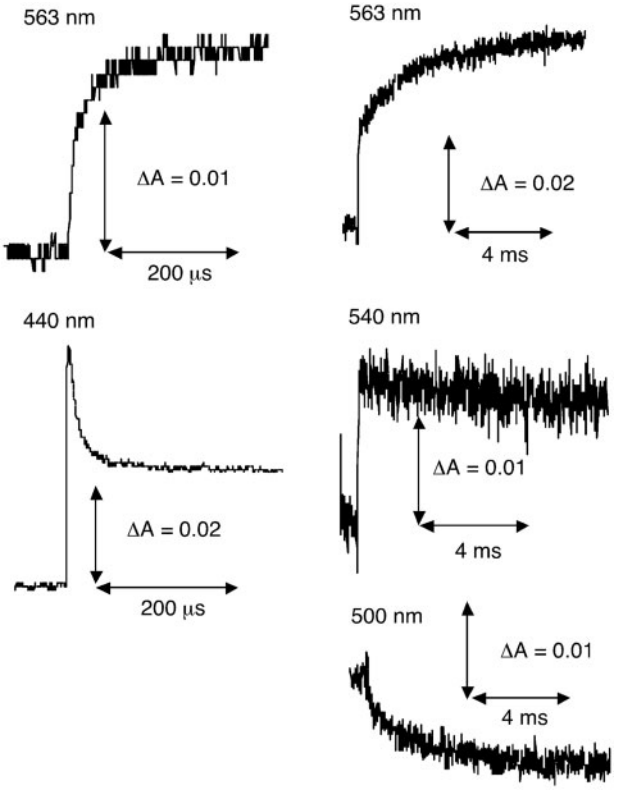

Fig. 1. **Absorbance changes in the His333Ala mutant enzyme after pulse radiolysis.** Pulse radiolysis was carried out in 10 mM potassium phosphate (pH 7.4) containing 2 mM NMA, 0.1% SML and 185 μM enzyme under unaerobic conditions.

RESULTS

Electron Transfer Process in the Cu_B-Deficient Mutant His333Ala—Pulse radiolysis experiments involve the almost instantaneous generation of NMA radical (E_m, –0.9 V), which in turn can reduce redox center(s) within a protein. As found for the wild-type enzyme (*11*), the NMA radical gave a rapid and specific reduction of the bound Q_8 at the Q_H site (E_m, ~0 mV) (*39*, *40*) in the His333Ala mutant (data not shown). The reduction of the bound Q_8 was almost stoichiometric with the concentration of NMA radical consumed, using the extinction coefficients of NMA radical ($\varepsilon_{420\ nm} = 3.2\ mM^{-1}\ cm^{-1}$) (*41*) and ubisemiquinone radical ($\varepsilon_{445\ nm} = 8.6\ mM^{-1}\ cm^{-1}$) (*42*). Thus, the absence of Cu_B, which is ligated by three histidines on helices VI and VII, do not affect the Q_H site at the periplasmic side of helices I and II (*4*).

Electron transfer from ubisemiquinone radical to hemes was monitored by absorbance changes at 440 (ubisemiquinone), and 563 nm (ferrous hemes *b* and *o*) (Fig. 1). In contrast to a monophasic reduction of hemes in the wild type ($1.5\times10^3\ s^{-1}$) (*43*), subsequent events following the initial rapid reduction of the bound Q_8 at the Q_H site were quite different in His333Ala. The decay of ubisemiquinone radical took place very rapidly with a half time of 10 μs at 440 nm (Fig. 1), whereas a similar process in the wild type occurred on the millisecond time scale (*11*). Furthermore, the reduction process of hemes in His333Ala occurred in two phases (Fig. 1). A faster phase was associated with the decay of ubisemiquinone radical. Only the faster increase and the slower decrease were observed at 540 and 500 nm, respectively.

Figure 2 shows the kinetic difference spectra at 0.05 and 10 ms after pulse radiolysis of the wild-type and His333Ala mutant enzymes. The spectrum of the wild-type 10 ms after pulse radiolysis was similar to the steady-state redox difference spectrum (Fig. 1A of ref. *44*). In His333Ala, the spectrum, corresponds to the faster phase, has a broad peak at ~560 nm and a shoulder at ~535 nm while the spectrum for the slower phase has an intense peak at 558 nm, accompanied by a broad trough around 480 nm. On the basis of properties of the α peak, these components are attributable to heme *b* and *o*, respectively (*45*). The lack of the heme *o*-Cu_B electromagnetic interactions in His333Ala could be the likely cause for the changes in spectroscopic properties of heme *o*.

An increase in the faster phase at 563 nm (heme *b*) and a decay at 440 nm (ubisemiquinone radical) followed first-order kinetics. The rate constants for the faster process and for the slower process were estimated to be 6.2×10^5 and $4.0\times10^2\ s^{-1}$, respectively. These rate constants were independent, within experimental error, of the enzyme concentration (data not shown). Therefore, we assume that the faster and the slower processes

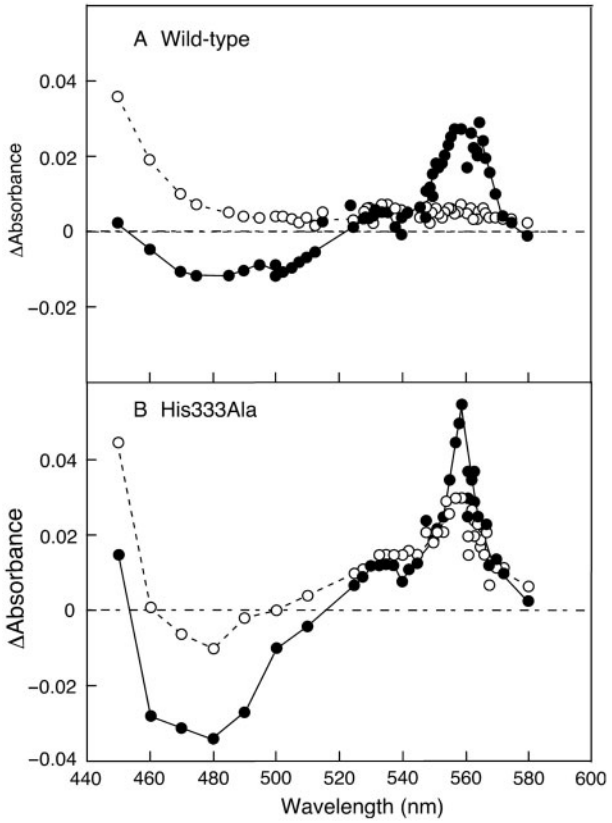

Fig. 2. **Kinetic difference spectra at 0.05 (open circle) and 10 ms (closed circle) after pulse radiolysis of the oxidized wild-type (A) and His333Ala mutant (B) enzymes.** The concentrations of the wild-type (A) and His333Ala (B) enzymes were 205 and 185 μM, respectively. Pulse radiolysis was carried out as described in the legend to Fig. 1.

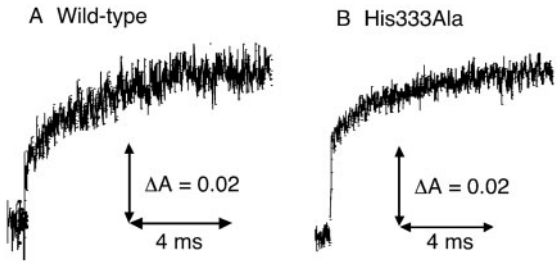

Fig. 3. **Absorbance changes at 561 nm in the oxidized wild-type and His333Ala enzymes after pulse radiolysis.** Pulse radiolysis was carried out as described in the legend to Fig. 1 in the presence of 1 mM KCN. The concentrations of the wild-type (A) and His333Ala (B) enzymes were 205 and 185 μM, respectively. Data were best fitted with a two-component model.

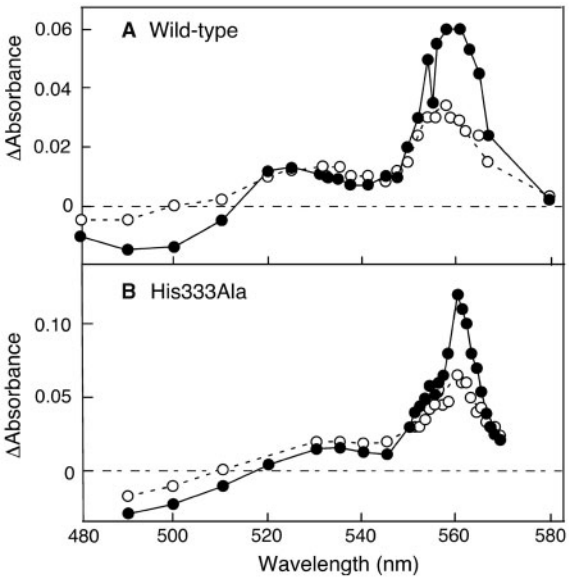

Fig. 4. **Kinetic difference spectra at 0.5 (open circle) and 10 ms (closed circle) after pulse radiolysis of the oxidized wild-type (A) and His333Ala mutant (B) enzymes in the presence of 1 mM KCN.** Pulse radiolysis was carried out as described in the legend to Fig. 3.

are intramolecular electron transfer from the ubisemiquinone radical to heme *b* and the heme *b*-to-heme *o* electron transfer, respectively.

Effect of KCN on Electron Transfer Processes in His333Ala—Upon addition of cyanide, a well-known respiration inhibitor, to the oxidized form of the respiratory terminal oxidases, cyanide binds to the dioxygen reduction site (*i.e.* heme *o* in cytochrome *bo* quinol oixdase and heme a_3 in cytochrome *c* oxidase) and forms the heme Fe(III)-CN-Cu_B(II) bridging structure (*37*). The lowering the redox potential of heme *o* by cyanide would suppress the heme *b*-to-heme *o* electron transfer in the wild-type enzyme. As in the case without cyanide, the bound Q_8 at the Q_H site was first reduced, and the subsequent intramolecular electron transfer occurs from ubisemiquinone to heme *o* through heme *b*. In the wild-type enzyme, the absorbance change at 561 nm showed a biphasic behaviour with the rate constants of 7×10^2 and $3\times10^2\,s^{-1}$ (Fig. 3). The kinetic difference spectrum in the faster phase (Fig. 4A), which has a broad α peak at ~560 nm, is essentially similar to that obtained in the faster phase of His333Ala mutant in the absence of cyanide (Fig. 2). On the other hand, the spectrum in the slower phase is similar to the fully reduced '*minus*' resting-oxidized redox difference spectrum (*44*). These findings confirm that the faster phase consists of the heme *b* reduction by intramolecular electron from the Q_H site, while the slower phase can be assigned to the reduction of heme *o*. Subsequently, cyanide bound to ferric heme *o* would be released upon the reduction of the wild-type enzyme (*46*), though this process is much slower than electron transfer processes. In contrast to the wild type, cyanide did not significantly affect the absorbance change at 561 nm in His333Ala (Fig. 4B), and the kinetic difference spectra were not different from those of the unliganded enzyme. Cyanide binding to ferric heme *o* in His333Ala was shown in steady-state binding experiments (*44*), but the binding affinity for cyanide may be altered in His333Ala. Cyanide binding to ferric heme *o* is rather slow process compared to electron transfer processes. In conclusion, effects of KCN on the heme reduction in the wild-type enzyme support that the His333Ala mutation slowed down the

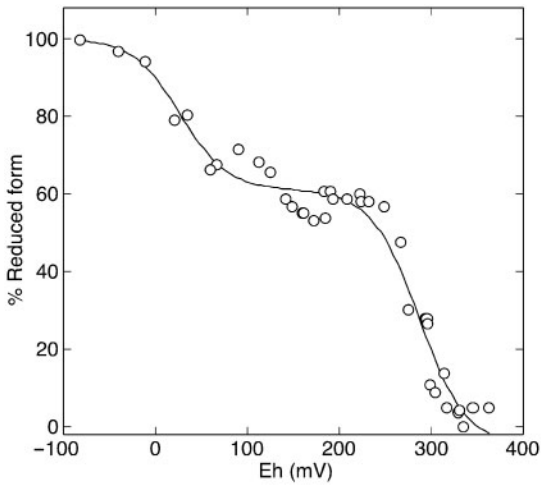

Fig. 5. **Potentiometric titration of the Soret peak of the His333Ala enzyme.** Data were best fitted by the two-component model with $E_{m1} = +28$ mV and $E_{m2} = +287$ mV. The concentrations of the His333Ala enzyme were 172 μM.

heme *b*-to-heme *o* electron transfer. It should be noted that the shape of the α peak in the slower phase of the wild type was broad as in the faster phase. The difference in the peak shape between the wild type and His333Ala could be due to a lack of electromagnetic interactions of heme *o* with Cu_B and/or microenvironmental changes around heme *o* in the mutant enzyme.

Potentiometric Analysis of Hemes in the His333Ala Mutant—It has been claimed that low-spin heme *b* contributes to most of the α absorption while the Soret absorption is a sum of equal contributions of low- and high-spin hemes (*45*). Due to heme *b*-heme *o* and heme *o*-Cu_B interactions in the wild-type enzyme (*47*), the titration curves for the α peak were composite and can be fitted by a two-component model with the E_m values of +67 and +123 mV (*39*). In the His333Ala mutant enzyme, the E_m values were shifted to +28 and +287 mV, respectively (Fig. 5). This indicates that a lack of magnetic interactions of heme *o* with Cu_B in His333Ala (*44*) resulted in the 40 mV decrease of the E_m value for heme *b* and the 160 mV increase of the E_m value for heme *o*. An increased energy gap between heme *b* and heme *o* is one of possible causes for the slower heme *b*-to-heme *o* electron transfer in the His333Ala mutant.

pH-Dependence of Intramolecular Electron Transfer Processes in the Cu_B-Deficient Mutant—To test the coupling of the intramolecular electron transfer to the proton uptake, we examined the pH-dependence of the heme reduction in the His333Ala mutant (Table 1). In the wild type, the rate for the heme *b* reduction decreased considerably with increasing external pH from 6.5 to 9.0 (*11*), due to the pH-dependence of the stability of ubisemiquinone anion radical (*40*). The rates for electron transfer from ubisemiquinone to heme *b* (k_1) and from ferrous heme *b* to ferric heme *o* (k_2) in the His333Ala mutant showed a pH dependence similar to the wild type (Table 1), suggesting that the absence of Cu_B and its coordinating OH^- (*48*) does not affect the uptake of the first chemical proton *via* K-channel.

Table 1. **pH-dependence of the rate constants of the heme reduction in the oxidized wild-type and His333Ala mutant enzymes monitored at 440 and 562 nm.**

Enzyme	pH	k_1 (s^{-1})	k_2 (s^{-1})
Wild type	6.0	1.6×10^3	ND[a]
	6.5	1.8×10^3	ND
	7.0	1.3×10^3	ND
	8.0	0.4×10^3	ND
	9.0	0.1×10^3	ND
His333Ala	5.6	$>6 \times 10^5$	1.1×10^3
	6.3	$>6 \times 10^5$	1.6×10^3
	7.0	5.0×10^5	0.9×10^3
	7.4	5.2×10^5	0.4×10^3
	8.2	1.5×10^5	0.4×10^3

[a]ND, not determined. The heme reduction in His333Ala contains two first-order rate constants, k_1 and k_2, attributable to the reduction of heme *b* and heme *o*, respectively.

DISCUSSION

Defects of Intramolecular Electron Transfer in His333Ala—Our results clearly showed that the heme *b*-to-heme *o* electron transfer in the His333Ala mutant ($4.0 \times 10^2\ s^{-1}$) deceased two-order of the magnitude from 2 to $5 \times 10^4\ s^{-1}$ of the wild-type enzyme (*8*, *43*, *49*). In His333Ala, electrons passed essentially quantitatively from heme *b* to heme *o* because the redox potentials of the two hemes differ by 260 mV (Fig. 5). In the wild type, on the other hand, the electron equilibrates between hemes *b* and *o*, driven by the 56-mV redox potential difference. In the wild-type enzyme, heme *o* and Cu_B are anti-ferromagnetically coupled, and the presence of interactions between hemes *b* and *o* has been suggested (*47*). A lack of such magnetic interactions between redox metal centres (*44*) and/or the absence of a copper ion (*48*) would affect the intramolecular one-electron transfer process in the His333Ala mutant enzyme.

Subunit I of His333Ala can bind one each of heme B and O molecules (*36*), as in the wild type (*37*). In the reduced-state, the wild-type enzyme shows the α and β peaks at ~563 and 531.5 nm, respectively. There are some uncertainty as to the contribution of hemes *b* and *o* to the visible absorption spectra. The spectral analysis of the wild-type enzyme in the presence of cyanide showed that high-spin heme *o* contributes only <10% to the reduced '*minus*' oxidized 560-nm band of the enzyme (*45*). On the other hand, we have shown in this study that the spectroscopic changes in the faster and slower phases account for the hemes *b* and *o* reduction, respectively. Since the electron transfer from heme *b* to heme *o* occurs quantitatively in the His333Ala mutant, we concluded that the characteristic feature of ferrous heme *b* exhibits a broad α and β peaks at ~560 and 540 nm whereas that of ferrous heme *o* has a sharp α peak at 558 nm with the β peak at 535 nm. Similar observations have been reported for heme ligand mutants (*44*). The 563.5-nm peak is diagnostic for low-spin heme *b*, and splits into 557 and 565 nm in the second-order finite difference spectrum at room temperature (data not shown). In the heme *b*-deficient mutants (His106Ala and His421Ala), the ferrous high-spin

heme *o* showed the sharp α peak at 558 nm (*44*). These observations suggest that the Q_H-to-heme *b* electron transfer in His333Ala is 100-fold faster than that of the wild type while the absence of Cu_B slows down 100-fold the heme *b*-to-heme *o* electron transfer.

Coupling of One-Electron Reduction of the Binuclear Centre and Uptake of the First Chemical Proton via K-Channel—Site-directed mutagenesis (*12–15*) and X-ray crystallographic (*4*, *16–18*) studies on bacterial heme-copper terminal oxidases suggest that D- and K-channels in subunit I are operative during redox-coupled proton pumping. Iwata *et al*. (*16*) proposed that D-channel, which is characterized by Asp135 (*E. coli* cytochrome *bo* numbering) and Glu286, participates in the translocation of four pumped protons while K-channel, which is characterized by Lys362 and Tyr288, delivers four chemical protons to the binuclear centre from the cytoplasm.

Upon reduction of the binuclear centre, the uptake of two chemical protons takes place to neutralize the increased negative charge within the oxidase (*20*), indicating the presence of proton acceptors in the oxidase. Electrostatic calculations (*50*) and Fourier transform infrared spectroscopic studies (*46*, *51–53*) indicate that Tyr288 and Glu286 in the vicinity of the binuclear centre are both protonated in the oxidized state. The X-ray crystallographic studies on the oxidized cytochrome *c* oxidase identified an electron density between heme a_3 iron and Cu_B, which has been interpreted as H_2O and OH^- bound to heme a_3 and Cu_B, respectively, in *Paracoccus denitrificans* (*48*), OH^- or H_2O in *Thermus thermophilus* (*17*) and *Rhodobacter sphaeroides* (*18*) and a bridging peroxide in bovine (*54*). Magnetic-circular-dichroism spectrum of the oxidized cytochrome *bo* indicates the presence of H_2O bound to heme *o* (*55*). Electron-nuclear double resonance (ENDOR) and Cu-extended X-ray absorption fine structure (EXAFS) studies on quinol oxidases from *E. coli* (*56*) and *Bacillus subtilis* (*57*) revealed that OH^- (or H_2O) coordinates to Cu_B in the oxidized enzyme. These results suggest that OH^- (or peroxide) bound to the binuclear centre would serve as a proton acceptor.

It is now assumed that K-channel delivers only one chemical proton to the binuclear centre at the initial reductive phase of dioxygen reduction, and D-channel translocates all other chemical and pumped protons (*12*, *25*, *26*, *58*, *59*). One-electron reduction of the oxidase results in the reduction of Cu_B (*58*), which is accompanied by uptake of one chemical proton via K-channel. The absence of OH^- coordinating to Cu_B(II) in the His333Ala mutant would affect the proton-coupled electron transfer to heme *o*. However, pH-dependence of the intramolecular electron transfer in the Cu_B-deficient mutant suggests that an electron was delivered to heme *o* and electron-coupled proton transfer may take place in His333Ala. Cu_B serves as a transient ligand-binding site during the delivery of exogenous ligands to the high-spin heme (*21*, *22*), and donates one electron to the bound dioxygen upon the O-O bond cleavage. In conclusion, this study indicates that Cu_B controls the E_m values of hemes *b* and *o* and is essential for the dioxygen reduction and the intramolecular electron transfer.

FUNDING

This work was supported in part by Grants-in-aid for Scientific Research (C) (20570124 to TM) and (B) (14380318 to KK) from the Japan Society for the Promotion of Science and for Scientific Research on Priority Areas (12147205 to KK) from the Ministry of Education, Culture, Sports, Science and Technology, Japan.

CONFLICT OF INTEREST

None declared.

ACKNOWLEDGEMENTS

We thank Robert B. Gennis (University of Illinois) for the *E. coli* strain GO103, Motonari Tsubaki (Kobe University) for valuable comments, and the members of the Radiation Laboratory in the Institute of Scientific and Industrial Research (Osaka University) for assistance in operating the linear accelerator.

REFERENCES

1. Trumpower, B.L. and Gennis, R.B. (1994) Energy transduction by cytochrome complexes in mitochondrial and bacterial respiration. *Annu. Rev. Biochem.* **63**, 675–716
2. Mogi, T., Tsubaki, M., Hori, H., Miyoshi, M., Nakamura, H., and Anraku, Y. (1998) Two terminal quinol oxidase families in *Escherichia coli*: variations on molecular machinery for dioxygen reduction. *J. Biochem. Mol. Biol. Biophys.* **2**, 79–110
3. Tsubaki, M., Hori, H., and Mogi, T. (2000) Probing molecular structure of dioxygen reduction site of bacterial quinol oxidases through ligand binding to the redox metal centers. *J. Inorg. Biochem.* **82**, 19–25
4. Abramson, J., Riistama, S., Larsson, G., Jasaitis, A., Svensson-Ek, M., Laakkonen, L., Puustinen, A., Iwata, S., and Wikström, M. (2000) The structure of the ubiquinol oxidase from *Escherichia coli* and its ubiquinone binding site. *Nat. Struct. Biol.* **7**, 910–917
5. Tsatsos, P.H., Reynolds, K., Nickels, E.F., He, D., Yu, C., and Gennis, R.B. (1998) Using matrix-assisted laser desorption ionization mass spectrometry to map the quinol binding site of cytochrome bo_3 from. *Escherichia coli*. *Biochemistry* **37**, 9884–9888
6. Ma, J., Puustinen, A., Wikström, M., and Gennis, R.B. (1998) Tryptophan-136 in subunit II of cytochrome bo_3 from *Escherichia coli* may participate in the binding of ubiquinol. *Biochemistry* **37**, 11806–11811
7. Sato-Watanabe, M., Mogi, T., Miyoshi, H., and Anraku, Y. (1998) Isolation and characterizations of quinone analogue-resistant mutants of *bo*-type ubiquinol oxidase from *Escherichia coli*. *Biochemistry* **37**, 12744–12752
8. Svensson-Ek, M. and Brzezinski, P. (1997) Oxidation of ubiquinol by cytochrome bo_3 from *Escherichia coli*: kinetics of electron and proton transfer. *Biochemistry* **36**, 5425–5431
9. Sato-Watanabe, M., Mogi, T., Miyoshi, H., and Anraku, Y. (1998) Characterization and functional role of the Q_H site of *bo*-type quinol oxidase from *Escherichia coli*. *Biochemistry* **37**, 5356–5361
10. Mogi, T., Sato-Watanabe, M., Miyoshi, H., and Orii, Y. (1999) Role of a bound ubiquinone on reactions of the *Escherichia coli* cytochrome *bo* with ubiquinol and dioxygen. *FEBS Lett.* **457**, 61–64
11. Kobayashi, K., Tagawa, S., and Mogi, T. (2000) Transient formation of ubisemiquinone radical and subsequent

electron transfer processes in the *Escherichia coli* cytochrome *bo* revealed by pulse radiolysis. *Biochemistry* **39**, 15620–15625
12. Konstantinov, A., Siletsky, S., Mitchell, D., Kaulen, A., and Gennis, R.B. (1997) The roles of the two proton input channels in cytochrome *c* oxidase from *Rhodobacter sphaeroides* probed by the effects of site-directed mutations on time-resolved electrogenic intraprotein proton transfer. *Proc. Natl Acad. Sci. USA* **94**, 9085–9090
13. Verkhovskaya, M.L., Garcia-Horsman, A., Puustinen, A., Rigaud, J., Morgan, J.E., Verkhovsky, M.I., and Wikström, M. (1997) Glutamic acid 286 in subunit I of cytochrome bo_3 is involved in proton translocation. *Proc. Natl Acad. Sci. USA* **94**, 10128–10131
14. Pfitzner, U., Hoffmeier, K., Harrenga, A., Kannt, A., Michel, H., Bamberg, E., Richter, O.H., and Ludwig, B. (2000) Tracing the D-pathway in reconstituted site-directed mutants of cytochrome *c* oxidase from *Paracoccus denitrificans*. *Biochemistry* **39**, 6756–6762
15. Lee, H., Das, T.K., Rousseau, D.L., Mills, D., Ferguson-Miller, S., and Gennis, R.B. (2000) Mutations in the putative H-channel in the cytochrome *c* oxidase from *Rhodobacter sphaeroides* show that this channel is not important for proton conduction but reveal modulation of the properties of heme *a*. *Biochemistry* **39**, 2989–2996
16. Iwata, S., Ostermeier, C., Ludwig, B., and Michel, H. (1995) Structure at 2.8 Å resolution of cytochrome *c* oxidase from *Paracoccus denitrificans*. *Nature* **376**, 660–669
17. Soulimane, T., Buse, G., Bourenkov, G.P., Bartunik, H.D., Huber, R., and Than, M.E. (2000) Structure and mechanism of the aberrant ba_3-cytochrome *c* oxidase from *Thermus thermophilus*. *EMBO J* **19**, 1766–1776
18. Svensson-Ek, M., Abramson, J., Larsson, G., Törnroth, S., Brzezinski, P., and Iwata, S. (2002) The X-ray crystal structures of wild-type and EQ(I-286) mutant cytochrome *c* oxidases from *Rhodobacter sphaeroides*. *J. Mol. Biol.* **321**, 329–339
19. Mitchell, R. and Rich, P.R. (1994) Proton uptake by cytochrome *c* oxidase on reduction and on ligand binding. *Biochim. Biophys. Acta* **1186**, 19–26
20. Karpefors, M., Ädelroth, P., Aagaard, A., Sigurdson, H., Svensson-Ek, M., and Brzezinski, P. (1998) Electron-proton interactions in terminal oxidases. *Biochim. Biophys. Acta* **1365**, 159–168
21. Dyer, R.B., Einarsdottir, Ó., Killough, P.M., López-Garriga, J.J., and Woodruff, W.H. (1989) Transient binding of photodissociated carbon monoxide to Cu_B^+ of eukaryotic cytochrome oxidase at ambient temperature. Direct evidence from time-resolved infrared spectroscopy. *J. Am. Chem. Soc.* **111**, 7657–7659
22. Lemon, D.D., Calhoun, M.W., Gennis, R.B., and Woodruff, W.H. (1993) The gateway to the active site of heme-copper oxidases. *Biochemistry* **32**, 11953–11956
23. Tomson, F.L., Bailey, J.A., Gennis, R.B., Unkefer, C.J., Li, Z., Silks, L.A., Martinez, R.A., Donohoe, R.J., Dyer, R.B., and Woodruff, W.H. (2002) Direct infrared detection of the covalently ring linked His-Tyr structure in the active site of the heme-copper oxidases. *Biochemistry* **41**, 14383–14390
24. Uchida, T., Mogi, T., and Kitagawa, K. (2004) Role of Tyr288 at the dioxygen reduction site of cytochrome *bo* studied by stable isotope labeling and resonance Raman spectroscopy. *J. Biol. Chem.* **279**, 53613–53620
25. Michel, H. (1998) Cytochrome *c* oxidase: catalytic cycle and mechanisms of proton pumping – a discussion. *Biochemistry* **38**, 15129–15140
26. Gennis, R.B. (1998) Multiple proton-conducting pathways in cytochrome oxidase and a proposed role for the active-site tyrosine. *Biochim. Biophys. Acta* **1365**, 241–248
27. Proshlyakov, D.A., Pressler, M.A., DeMaso, C., Leykam, J.F., DeWitt, D.L., and Babcock, G.T. (2000) Oxygen activation and reduction in respiration: involvement of redox-active tyrosine 244. *Science* **290**, 1588–1591
28. Blomberg, M.R.A., Siegbahn, P.E.M., Babcock, G.T., and Wikström, M. (2000) O–O bond splitting mechanism in cytochrome oxidase. *J. Inorg. Biochem.* **80**, 261–269
29. Uchida, T., Mogi, T., and Kitagawa, T. (2000) Resonance Raman studies of oxo intermediates in the reaction of pulsed cytochrome *bo* with hydrogen peroxide. *Biochemistry* **39**, 6669–6678
30. Kobayashi, K., Une, K., and Hayashi, K. (1989) Electron transfer process in cytochrome oxidase after pulse radiolysis. *J. Biol. Chem.* **264**, 7976–7980
31. Kobayashi, K., Tagawa, S., and Mogi, T. (1999) Pulse radiolysis studies on electron transfer processes in cytochrome *bd*-type ubiquinol oxidase from *Escherichia coli*. *Biochemistry* **38**, 5913–5917
32. Kobayashi, K., Koppenhöfer, A., Ferguson, S.J., Watmough, N.J., and Tagawa, S. (2001) Intramolecular electron transfer from *c* heme to d_1 heme in bacterial cytochrome cd_1 nitrite reductase occurs over the same distance at very different rates depending on the source of the enzyme. *Biochemistry* **40**, 8542–8547
33. Kobayashi, K., Tagawa, S., Daff, S., Sagami, I., and Shimizu, T. (2001) Rapid calmodulin-dependent interdomain electron transfer in neuronal nitric-oxide synthase measured by pulse radiolysis. *J. Biol. Chem.* **276**, 39864–39871
34. Kobayashi, K., Miki, M., Okamoto, K., and Nishino, T. (1993) Electron transfer process in milk xanthine dehydrogenase as studied by pulse radiolysis. *J. Biol. Chem.* **268**, 24642–24646
35. Kritsis, P., Messerschmidt, A., Huber, R., Salmon, A., and Sykes, A.G. (1993) Pulse-radiolysis studies on the oxidised form of the multicopper enzyme ascorbate oxidase: evidence for two intramolecular electron-transfer steps. *J. Chem. Soc., Dalton Trans*, 731–735
36. Mogi, T., Hirano, T., Nakamura, H., Anraku, Y., and Orii, Y. (1995) Cu_B promotes both binding and reduction of dioxygen at the heme-copper binuclear center in the *Escherichia coli bo*-type ubiquinol oxidase. *FEBS Lett.* **370**, 259–263
37. Tsubaki, M., Mogi, T., Anraku, Y., and Hori, H. (1993) Structure of heme-copper binuclear center of the cytochrome *bo* complex of *Escherichia coli*: EPR and Fourier-transform infrared spectroscopic studies. *Biochemistry* **32**, 6065–6072
38. Dutton, P.L. (1978) Redox potentiometry: determination of midpoint potentials of oxidation-reduction components of biological electron-transfer systems. *Methods Enzymol.* **54**, 411–435
39. Sato-Watanabe, M., Itoh, S., Mogi, T., Matsuura, K., Miyoshi, H., and Anraku, Y. (1995) Stabilization of a semiquinone radical at the high affinity quinone binding site of the *Escherichia coli bo*-type ubiquinol oxidase. *FEBS Lett.* **374**, 265–269
40. Ingledew, W.J., Ohnishi, T., and Salerno, J.C. (1995) Studies on a stabilisation of ubisemiquinone by *Escherichia coli* quinol oxidase, cytochrome *bo*. *Eur. J. Biochem.* **227**, 903–908
41. Hill, R. and Anderson, R.F. (1991) Electron transfer in milk xanthine oxidase as studied by pulse radiolysis. *J. Biol. Chem.* **266**, 5608–5615
42. Land, E.J., Simic, M., and Swallow, A.J. (1971) Optical absorption spectrum of half-reduced ubiquinone. *Biochim. Biophys. Acta* **226**, 239–240
43. Orii, Y., Mogi, T., Kawasaki, M., and Anraku, Y. (1994) Facilitated intramolecular electron transfer in the cytochrome *bo*-type ubiquinol oxidase initiated upon reaction of the fully-reduced enzyme with dioxygen. *FEBS Lett.* **352**, 151–154
44. Tsubaki, M., Mogi, T., Hori, H., Ogura, T., Hirota, S., Kitagawa, T., and Anraku, Y. (1994) Molecular structure of redox metal centers of the cytochrome *bo* complex from

Escherichia coli: spectroscopic characterizations of the subunit I histidine mutant oxidases. *J. Biol. Chem.* **269**, 30861–30868

45. Puustinen, A., Morgan, J.E., Verkovsky, M., Gennis, R.B., and Wikström, M. (1992) The low-spin heme site of cytochrome *o* from *Escherichia coli* is promiscuous with respect to heme type. *Biochemistry* **31**, 10363–10369
46. Salerno, J.C., Bolgiano, B., Poole, R.K., Gennis, R.B., and Ingledew, W.J. (1990) Heme-copper and heme-heme interactions in the cytochrome *bo*-containing quinol oxidase of *Escherichia coli*. *J. Biol. Chem.* **265**, 4364–4368
47. Ostermeier, C., Harrenga, A., Ermler, U., and Michel, H. (1997) Structure at 2.7 Å resolution of the *Paracoccus denitrificans* two-subunit cytochrome *c* oxidase complexed with an antibody F_V fragment. *Proc. Natl Acad. Sci. USA* **94**, 10547–10553
48. Hirota, S., Mogi, T., Ogura, T., Hirano, T., Anraku, Y., and Kitagawa, T. (1994) Observation of the Fe-O_2 and $Fe^{IV}=O$ Raman bands in dioxygen reduction by cytochrome *bo*-type ubiquinol oxidase from *Escherichia coli*. *FEBS Lett.* **352**, 67–70
49. Kannt, A., Lancaster, C.R.D., and Michel, H. (1998) The coupling of electron transfer and proton translocation: electrostatic calculations on *Paracoccus denitrificans* cytochrome *c* oxidase. *Biophys. J* **74**, 708–721
50. Yamazaki, Y., Kandori, H., and Mogi, T. (1999) Effects of amino acid substitutions on redox-induced conformational changes of the *Escherichia coli bo*-type ubiquinol oxidase revealed by Fourier-transform infrared spectroscopy. *J. Biochem.* **126**, 194–199
51. Hellwig, P., Behr, J., Ostermeier, C., Richter, O.H., Pfitzner, U., Odenwald, A., Ludwig, B., Michel, H., and Mäntele, W. (1998) Involvement of glutamic acid 278 in the redox reaction of the cytochrome *c* oxidase from *Paracoccus denitrificans* investigated by FTIR spectroscopy. *Biochemistry* **37**, 7390–7399
52. Lübben, M., Prutsch, A., Mamat, B., and Gerwert, K. (1999) Electron transfer induces side-chain conformational changes of glutamate-286 from cytochrome bo_3. *Biochemistry* **38**, 2048–2056
53. Nyquist, R.M., Heitbrink, D., Bolwien, C., Gennis, R.B., and Heberle, J. (2003) Direct observation of protonation reactions during the catalytic cycle of cytochrome *c* oxidase. *Proc. Natl Acad. Sci. USA* **100**, 8715–8720
54. Yoshikawa, S., Shinzawa-Itoh, K., Nakashima, R., Yaono, R., Yamashita, E., Inoue, N., Yao, M., Fei, M.J., Libei, C.P., Mizushima, T., Yamaguchi, H., Tomizaki, T., and Tsukihara, T. (1998) Redox-coupled crystal structural changes in bovine heart cytochrome *c* oxidase. *Science* **280**, 1723–1729
55. Cheeseman, M.R., Watmough, N.J., Gennis, R.B., Greenwood, C., and Thomson, A.J. (1994) Magnetic-circular-dichroism studies of *Escherichia coli* cytochrome *bo*. *Eur. J. Biochem.* **219**, 595–602
56. Osborne, J.P., Cosper, N.J., Stälhandske, C.M.V., Scott, R.A., Alben, J.O., and Gennis, R.B. (1999) Cu XAS shows a change in the ligation of Cu_B upon reduction of cytochrome bo_3 from *Escherichia coli*. *Biochemistry* **38**, 4526–4532
57. Fann, Y.C., Ahmed, I., Blackburn, N.J., Boswell, J.S., Verkhovskaya, M.L., Hoffman, B.M., and Wikström, M. (1995) Structure of Cu_B in the binuclear heme-copper center of the cytochrome aa_3-type quinol oxidase from *Bacillus subtilis*: an ENDOR and EXAFS study. *Biochemistry* **34**, 10245–10255
58. Wikström, M., Jasaitis, A., Backgren, C., Puustinen, A., and Verkovsky, M.I. (2000) The role of the D- and K-pathways of proton transfer in the function of the haem–copper oxidases. *Biochim. Biophys. Acta* **1459**, 514–520
59. Ruitenberg, M., Kannt, A., Bamberg, E., Ludwig, B., Michel, H., and Fendler, K. (2000) Single-electron reduction of the oxidized state is coupled to proton uptake via the K pathway in *Paracoccus denitrificans* cytochrome *c* oxidase. *Proc. Natl Acad. Sci. USA* **97**, 4632–4636